Chemical Engineering Science 61 (2006) 182–191

Chemical Engineering Science

www.elsevier.com/locate/ces

A population balance model for flocculation of colloidal suspensions by polymer bridging

Venkataramana Runkana[a, b], P. Somasundaran[a, *], P.C. Kapur[b]

[a] NSF Industry/University Cooperative Research Center for Advanced Studies in Novel Surfactants, School of Engineering and Applied Science, Columbia University, New York, NY 10027, USA

[b] Tata Research Development and Design Centre, 54-B, Hadapsar Industrial Estate, Pune, 411013 India

Received 1 June 2004; accepted 1 January 2005
Available online 6 July 2005

Abstract

A detailed population balance model for flocculation of colloidal suspensions by polymer bridging under quiescent flow conditions is presented. The collision efficiency factor is estimated as a function of interaction forces between polymer coated particles. The total interaction energy is computed as a sum of van der Waals attraction, electrical double layer repulsion and bridging attraction or steric repulsion due to adsorbed polymer. The scaling theory is used to compute the forces due to adsorbed polymer and the van der Waals attraction is modified to account for presence of polymer layer around a particle. The irregular structure of flocs is taken into account by incorporating the mass fractal dimension of flocs. When tested with experimental floc size distribution data published in the literature, the model predicts the experimental behavior adequately. This is the first attempt towards incorporating theories of polymer-induced surface forces into a flocculation model, and as such the model presented here is more general than those proposed previously.

Keywords: Population balance; Flocculation; Colloids; Surface forces; Fractals; Polymers

1. Introduction

Flocculation of colloidal suspensions is an important unit operation in many industries such as pulp and papermaking (Pelton, 1999), mineral processing (Somasundaran et al., 1996) and water treatment (Thomas et al., 1999). Polymers and polyelectrolytes, inorganic salts and surfactants are routinely used to either flocculate or disperse a suspension. Flocculation by polymers is a complex phenomenon, which involves several steps or sub-processes occurring sequentially or concurrently. These include (Gregory, 1988): (i) mixing of particles and polymers in solution, (ii) adsorption of polymer chains on particle surface, (iii) reconformation of adsorbed chains on the surface, (iv) formation of aggregates, (v) restructuring of flocs, and (vi) subsidence, or sedimentation of flocs. Polymers and polyelectrolytes are common additives for controlling stability as well as rate of sedimentation of flocculating suspensions. These changes are brought about by altering polymer adsorption and conformation at the solid-solution interface by manipulating a number of variables such as pH, ionic strength, polymer concentration and temperature.

The key variable in flocculation is floc size distribution (FSD) as it influences rate of floc sedimentation and suspension turbidity. It is a complex function of several process variables including initial or feed particle size distribution, solution pH, electrolyte concentration, temperature, polymer concentration and its molecular weight distribution. Population balances have been applied extensively for modeling flocculation and for predicting the evolution of FSD with time. The two important parameters in the flocculation model are collision frequency factor and collision efficiency factor. Depending on the process operating conditions and material properties, aggregation takes place by one or more of the following mechanisms: perikinetic aggregation,

* Corresponding author. Fax: +1 212 854 8362.
E-mail address: ps24@columbia.edu (P. Somasundaran).

0009-2509/$ - see front matter © 2005 Elsevier Ltd. All rights reserved.
doi:10.1016/j.ces.2005.01.046

orthokinetic aggregation and differential sedimentation. Appropriate equations or kernels are included in the flocculation model to capture the mode and frequency of particle and/or aggregate encounters. Collision efficiency, on the other hand, has been mostly employed as a fitting parameter, even though it is actually a function of the interaction forces between particles which, in turn, depend critically on the type of flocculant used. Because collision efficiency factor is treated as a fitting parameter, the population balance models are restricted in their applicability to specific processes.

Flocculation in presence of polymers can occur by any one or more of the four well-known mechanisms: simple charge neutralization, charge patch neutralization, polymer bridging and polymer depletion (Napper, 1983; Levine and Friesen, 1987). The first three mechanisms take place due to polymer adsorption while depletion occurs in the presence of nonadsorbing polymers. In an earlier paper, we presented a discretized population balance model for flocculation of colloidal suspensions by simple charge neutralization in presence of inorganic electrolytes or polymers (Runkana et al., 2004). Here we extend the treatment for bridging flocculation under quiescent flow conditions by incorporating a collision efficiency model, which takes into account bridging attraction or steric repulsion, van der Waals attraction and electrical double layer repulsion between particles. The objective is to predict the evolution of FSD preferably or at the minimum, mean floc diameter with time as a function of important flocculation process variables. It is of course recognized that mean diameter may not furnish a definitive validation of the model and FSD data are required for a more authentic validation.

2. Bridging flocculation model

2.1. Population balance equation

The starting point of our model is the discretized and geometrically sectioned population balance equation (PBE) proposed by Hounslow et al. (1988) for modeling aggregation. The rate of change of particle or floc concentration due to aggregation alone is given by Hounslow et al. (1988)

$$\begin{aligned}\frac{\mathrm{d}N_i}{\mathrm{d}t} &= N_{i-1}\sum_{j=1}^{i-2} 2^{j-i+1}\alpha_{i-1,j}\,\beta_{i-1,j}N_j \\ &\quad + \frac{1}{2}\,\alpha_{i-1,i-1}\beta_{i-1,i-1}N_{i-1}^2 \\ &\quad - N_i\sum_{j=1}^{i-1} 2^{j-i}\alpha_{i,j}\beta_{i,j}N_j \\ &\quad - N_i\sum_{j=i}^{\max}\alpha_{i,j}\beta_{i,j}N_j, \qquad (1)\end{aligned}$$

where N_i is number concentration of particles or flocs in section i, t is flocculation time β is collision frequency factor and α is collision efficiency factor. The first term on the right-hand side accounts for growth of aggregates in section i due to aggregation of clusters that belong to sections smaller than i, except the immediately adjacent smaller section. The second term represents growth due to aggregation of clusters belonging to the immediately adjacent smaller section. The third term describes loss of aggregates in section i due to their interaction with entities belonging to smaller sections and the fourth term represents loss of aggregates due to aggregation of clusters in section i and their interactions with aggregates belonging to sections larger than i. The smallest section corresponds to primary particles and the section designated max contains aggregates of largest characteristic volume. Details of discretizing the PBE and lumping of size classes are available elsewhere (Spicer and Pratsinis, 1996; Runkana et al., 2004).

2.2. Collision frequency

Aggregation occurs by particle–particle, particle–cluster and cluster–cluster collisions followed by the formation of flocs, which are highly irregular in shape and structure. The irregular structure of flocs is taken into account by explicitly incorporating the mass fractal dimension of flocs into the expression for collision frequency factor. The rate of flocculation is primarily a function of collision frequency if the forces of attraction between particles dominate the forces of repulsion. The collision frequency depends strongly on particle (or aggregate) collision radius, which increases due to adsorption of polymer chains on the surface. Its magnitude depends on adsorbed layer thickness, which is determined by polymer adsorption density and conformation at the solid–liquid interface.

Adsorption of polymers at the solid–liquid interface is a complex phenomenon and depends on various factors such as polymer concentration in solution and at the interface, polymer molecular weight and charge density distribution, nature of solvent, surface charge density distribution, pH, temperature and type and concentration of electrolyte species present in solution (Fleer et al., 1993). Polymer adsorption on particles occurs by collisions between particles and polymer chains. In absence of any applied shear, these collisions also take place under Brownian motion. The process essentially involves three steps: diffusion of polymer chains from bulk solution to the interface, attachment of polymer segments to surface sites and relaxation or reorientation of polymer chains at the interface (Cohen Stuart and Fleer, 1996). Adsorption of polymers on oppositely charged surfaces is generally fast, strong and irreversible. Moreover, polymer relaxation times are of the order of few seconds (van de Ven, 1994). Hence, it is reasonable to assume that polymer attains its equilibrium conformation before particles undergo any meaningful number of collisions.

Depending on the affinity of the polymer to the surface, polymer chains can have one or a combination of three

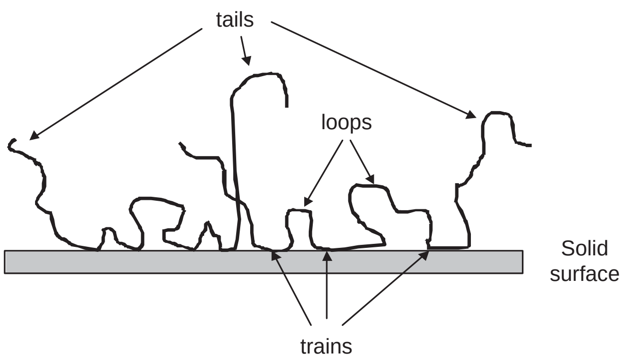

Fig. 1. Schematic representation of polymer conformation at the solid–liquid interface.

conformations shown in Fig. 1, namely, trains (stretched on the surface), loops (coils), and tails (stretched or dangling into the solution at some angle to the surface) (Tjipangandjara et al., 1990; Fleer et al., 1993). Polymer conformation is a function of almost all the flocculation process variables enumerated earlier and determines the mechanism by which flocculation occurs. For example, when the polymer adsorbs in the form of trains, the number of contacts between polymer backbone and surface is high and the adsorbed layer thickness is low, resulting in flocculation by simple charge neutralization (Zhang and Buffle, 1995). The rate of flocculation is comparable to that obtained with commonly employed inorganic coagulants. In the case of bridging, the adsorbed layer thickness is quite high and results in high collision radii. This is the reason for high rates of flocculation observed with high molecular weight polymers (Yu and Somasundaran, 1996).

In absence of applied shear, aggregation occurs by Brownian motion and differential sedimentation of flocs. The collision frequency factor $\beta_{i,j}$ is assumed to be a sum of contributions by these two mechanisms. The collision frequency factor for flocculation by perikinetic aggregation of entities belonging to sections i and j is (Smoluchowski, 1916)

$$\beta_{i,j}^{\mathrm{Br}} = \frac{2k_B T}{3\mu}\left(\frac{1}{r_{c_i}} + \frac{1}{r_{c_j}}\right)(r_{c_i} + r_{c_j}) \tag{2}$$

and for aggregation by differential sedimentation (Camp and Stein, 1943):

$$\beta_{i,j}^{DS} = \frac{2\pi g}{9\mu}(r_{c_i} + r_{c_j})^2 |r_{c_i}^2(\rho_i - \rho_l) - r_{c_j}^2(\rho_j - \rho_l)|, \tag{3}$$

where k_B is Boltzmann constant, T is suspension temperature, μ is dynamic viscosity of the suspending fluid, r_{c_i} and r_{c_j} are collision radii of particles or aggregates belonging to sections i and j, respectively, ρ_i and ρ_l are densities of aggregate and fluid, respectively, and g is acceleration due to gravity. The collision radius of an aggregate, r_{c_i} containing n_0 monodisperse primary particles is given by Flesch et al. (1999)

$$r_{c_i} = r_0\left(\frac{n_{0_i}}{C_L}\right)^{1/d_F}, \tag{4}$$

where C_L is aggregate structure prefactor, r_0 is composite radius of a particle with adsorbed polymer layers and d_F is mass fractal dimension of an aggregate, which is a complex function of flocculation process variables such as pH, temperature, initial or feed particle size distribution, ionic strength, polymer molecular weight and its concentration (Klimpel and Hogg, 1986; Zhang and Buffle, 1995). The composite particle radius is estimated by adding adsorbed layer thickness to the solid particle radius. The aggregate density ρ_i, which decreases as size increases, can be estimated by the following equation (Jiang and Logan, 1991):

$$\rho_i = \rho_0\left(\frac{r_{c_i}}{r_0}\right)^{d_F-3}, \tag{5}$$

where ρ_0 is density of primary particles. This equation is applicable mainly in the linear part of the aggregate size-density curve.

2.3. Collision efficiency

The collision efficiency factor for aggregates is computed as reciprocal of the modified Fuchs' stability ratio W for two primary particles k and l (Fuchs, 1934; Derjaguin and Muller, 1967; McGown and Parfitt, 1967; Spielman, 1970):

$$W_{k,l} = \frac{\int_{r_{0_k}+r_{0_l}}^{\infty} D_{k,l}(\exp(V_T/k_B T)/s^2)\,\mathrm{d}s}{\int_{r_{0_k}+r_{0_l}}^{\infty} D_{k,l}(\exp(V_{vdW}/k_B T)/s^2)\,\mathrm{d}s}, \tag{6}$$

where $D_{k,l}$ is hydrodynamic correction factor, given by Honig et al. (1971)

$$D_{k,l} = \frac{6\bar{h}_0^2 + 13\bar{h}_0 + 2}{6\bar{h}_0^2 + 4\bar{h}_0} \tag{7}$$

and V_T is total energy of interaction and V_{vdW} is van der Waals energy of attraction between two primary particles of radii r_{0_k} and r_{0_l} (assumed spherical), s is distance between particle centers ($s = r_{0_k} + r_{0_l} + h_0$), h_0 is distance of closest approach between particle surfaces and $\bar{h}_0 = 2h_0/(r_{0_k} + r_{0_l})$ is normalized distance. It is assumed that efficiency of aggregate collisions depends mainly on the interaction between particles lying on the surface of the aggregates. The forces between particles drop rapidly with distance and, as such, interaction between aggregates can be approximated by interaction between the surface particles (Firth and Hunter, 1976).

2.4. Interaction forces between polymer-coated particles

The electrochemical nature of particle surface changes due to adsorption of polymers and polyelectrolytes. The adsorbed polymer chains introduce steric and bridging forces in addition to perturbing van der Waals attraction and electrostatic repulsion. The van der Waals attraction is affected because dielectric constant and refractive index of the polymer are different from those of the solvent. The surface potential increases or decreases depending on polymer charge density distribution. Moreover, the range over which particle–particle interaction occurs also changes depending on the thickness of the adsorbed layer, especially tail length in case of dangling polymer chains in the solution. The total interaction energy between particles with adsorbed polymer layers is computed by applying the usual assumption of additivity. It is recognized that the assumption of each force acting individually, neither influencing nor getting influenced by other forces present, is a gross simplification. However, in absence of sufficient understanding of how the forces influence each other, we are obliged to invoke the simple addition assumption in the model formulation.

The van der Waals attraction V_{vdW} is computed using the model originally proposed by Vold (1961) for identical particles covered with adsorbed layers. Subsequently, Vincent (1973) generalized Vold's expression for two dissimilar solids and polymers, which simplifies to Vold's expression for two solids of same kind having equal thickness of adsorbed layer. The expression of Vincent is

$$\begin{aligned} -12V_{vdW} = {} & H_{s_k s_l}(A_{s_k}^{1/2} - A_m^{1/2})(A_{s_l}^{1/2} - A_m^{1/2}) \\ & + H_{p_k p_l}(A_{p_k}^{1/2} - A_{s_k}^{1/2})(A_{p_l}^{1/2} - A_{s_l}^{1/2}) \\ & + H_{p_k s_l}(A_{p_k}^{1/2} - A_{s_k}^{1/2})(A_{s_l}^{1/2} - A_m^{1/2}) \\ & + H_{p_l s_k}(A_{p_l}^{1/2} - A_{s_l}^{1/2})(A_{s_k}^{1/2} - A_m^{1/2}), \end{aligned} \tag{8}$$

where A_p, A_m and A_s are Hamaker constants of solids, solvent and polymer, respectively, across a vacuum. The unretarded geometric function $H(x, y)$ is (Hamaker, 1937)

$$\begin{aligned} H(x, y) = {} & \frac{y}{x^2 + xy + x} + \frac{y}{x^2 + xy + x + y} \\ & + 2\ln\left[\frac{x^2 + xy + x}{x^2 + xy + x + y}\right], \end{aligned} \tag{9}$$

where $x = \Delta/2R_k$ and $y = R_l/R_k$. Expressions for Δ, R_k and R_l for different H functions in Eq. (8) are given elsewhere (Vincent, 1973). Eq. (8) does not take into account the retardation phenomenon, which sets in at about 5 nm from the particle surface (Israelachvili, 1991). We incorporate the retardation effect by multiplying unretarded van der Waals attraction with a correction function proposed by Gregory (1981).

For estimating electrical double layer repulsion V_{edl} between two spherical particles having surface potentials, ψ_{0_k} and ψ_{0_l}, we employ the following analytical expression proposed by Bell et al. (1970)

$$\begin{aligned} V_{edl} = {} & 64\pi\varepsilon_r\varepsilon_0\left(\frac{k_B T}{z_c e}\right)^2\left(\frac{r_{0_k} r_{0_l}}{r_{0_k} + r_{0_l}}\right)\tanh\left(\frac{z_c e\psi_{0_k}}{4k_B T}\right) \\ & \times \tanh\left(\frac{z_c e\psi_{0_l}}{4k_B T}\right)\exp(-\kappa h_0), \end{aligned} \tag{10}$$

where e is elementary charge and z_c is valence of the counterion and ε_0 and ε_r are dielectric constants of vacuum and solvent, respectively. The Debye–Huckel parameter κ is a function of electrolyte concentration, valence of electrolyte ions and temperature. The surface potential depends on pH, temperature, type and concentration of electrolyte and concentration, molecular weight and charge density of polymer (Tjipangandjara et al., 1990; Zhang and Buffle, 1995).

The scaling theory (de Gennes, 1981, 1982) is used to compute forces due to adsorbed polymer layers. It was chosen because it permits derivation of analytical formulas for interaction between spherical particles. The number of parameters needed in this approach is also quite small. These can be obtained experimentally, in principle at least. The scaling theory is based on minimization of a surface free energy functional subject to the constraint that total amount of polymer adsorbed is fixed in the region between two surfaces having adsorbed layers. The form of the surface energy functional depends on nature of solvent and polymer concentration. The scaling theory for good solvents is selected in the present work. The surface free energy functional is assumed to be a sum of two contributions, a surface term to account for the interaction between polymer and surface, and a bulk contribution due to variation of polymer concentration from the surface (de Gennes, 1982):

$$\begin{aligned} \gamma^S - \gamma_0^S = {} & -|\gamma_1^S|\Phi_s + \alpha_{Sc} k_B T \\ & \times \int_0^{h_0} \frac{1}{\xi^3(\Phi)}\left[1 + \left(m_0\,\frac{\xi(\Phi)}{\Phi}\frac{\mathrm{d}\Phi}{\mathrm{d}z}\right)^2\right]\mathrm{d}z, \end{aligned} \tag{11}$$

where γ^S and γ_0^S are surface free energy of polymer solution and of pure solvent, respectively. γ_1^S is local solute–interface interaction energy per unit area. It is negative for adsorbing surfaces. $\Phi(z)$ is polymer volume fraction at a distance z from the surface and $\Phi_S = \Phi(z=0)$. α_{Sc} and m_0 are numerical constants, which can be obtained from osmotic pressure and light scattering experiments on polymer solutions. ξ is termed as correlation length and represents the average distance between two successive contacts of a polymer chain with other chains. The constant α_{Sc} is related to osmotic pressure of a semidilute solution (de Gennes, 1982). It can also be obtained from data on forces between two surfaces by assuming that the osmotic pressure between two surfaces is essentially equal to the intersurface pressure (Klein and Rossi, 1998). Recently Klein and Rossi (1998) found an important result for applying the scaling theory for predicting interaction forces between polymer-covered surfaces in good solvents. The surface energy functional, given above is for a single surface and gradient term in the integral accounts for

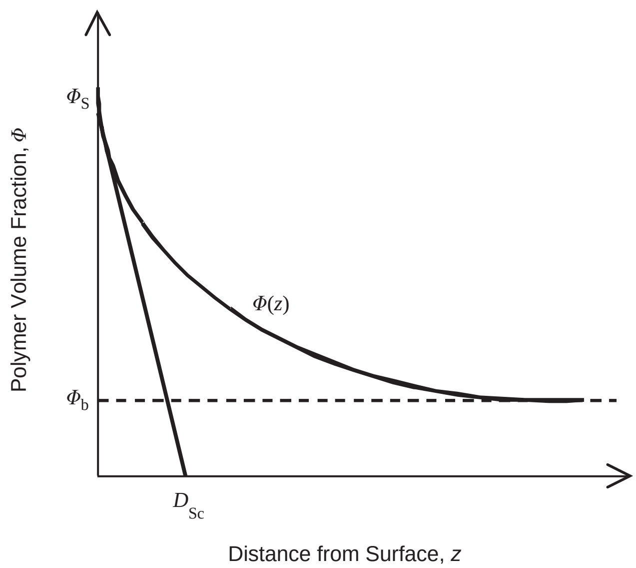

Fig. 2. Typical distribution profile of polymer at the solid–liquid interface.

variations in polymer concentration from the surface. It is normally assumed that a symmetric profile of polymer concentration develops when two surfaces are brought in proximity of each other. The concentration is maximum at the interface and gradually decreases to a minimum bulk value at the midpoint. However, if the separation distance between surfaces is decreased further, the concentration profiles will overlap and eventually, at very short surface separations, polymer concentration in the gap will reach a uniform level. In other words, $\Phi(z) \approx \Phi_s \approx \Phi_m \approx \Gamma a_m^3/h_0$, where Φ_s and Φ_m are polymer concentrations at the surface and midpoint between the surfaces, respectively, a_m is effective monomer size and Γ is total amount of polymer adsorbed on a single surface. In this case, the gradient term in Eq. (11) can be neglected resulting in the following simple relationship (Klein and Rossi, 1998):

$$\gamma^S - \gamma_0^S \approx -|\gamma_1^S|\Phi_s + \frac{\alpha_{Sc} k_B T}{a_m^3} h_0 \Phi_m^{9/4}. \tag{12}$$

The intersurface pressure Π_d can be derived as a function of surface separation from Eq. (12) (Klein and Rossi, 1998):

$$\begin{aligned}\Pi_d &= -\frac{\partial(2\gamma^S)}{\partial(2h_0)} = -\frac{\partial\gamma^S}{\partial h_0} = -\frac{2}{D_{Sc}}\frac{\partial\gamma^S}{\partial\omega_{Sc}} \\ &\approx \left(\frac{\alpha_{Sc}k_BT}{a_m^3}\right)\Phi_{s0}^{9/4}\left[-\frac{32\Gamma}{\omega_{Sc}^2\Gamma_0} + \frac{5}{4}\left(\frac{8\Gamma}{\omega_{Sc}\Gamma_0}\right)^{9/4}\right],\end{aligned} \tag{13}$$

where Γ_0 is adsorbed amount at saturation, ω_{Sc} is reduced length, defined as $\omega_{Sc} = 2h_0/D_{Sc}$, Φ_{s0} is polymer concentration at a single saturated surface and D_{Sc} is referred to as the scaling length (Fig. 2). It is a measure of segment-surface attraction and is related to γ_1^S (de Gennes, 1982). Both Φ_{s0} and D_{Sc} can be obtained from polymer volume fraction profiles measured by neutron scattering and reflectometry.

Eq. (13) is applicable to flat surfaces. The interaction energy between two spherical polymer-covered particles can be derived from it in two steps (Runkana, 2003) by first integrating the equation for intersurface pressure (Eq. (13)) to obtain interaction energy between flat surfaces and then applying the Derjaguin approximation (Derjaguin, 1934):

$$V_S^{ES}(h, r_{0_k}) = \pi r_{0_k} \int_{h_0}^{2\delta} V_S^{FP}(h)\,\mathrm{d}h, \tag{14}$$

where V_S^{ES} and V_S^{FP} are interaction energies for spheres of equal radii and for flat surfaces, respectively, h is surface separation and δ is adsorbed layer thickness. Integration of Eq. (13) yields the following expression for V_S^{FP}:

$$\begin{aligned}V_S^{FP} = &\left(\frac{\alpha_{Sc}k_BT}{a_m^3}\right)\Phi_{s0}^{9/4}D_{Sc} \\ &\times\left[-\frac{16\Gamma D_{Sc}}{h_0\Gamma_0} + \frac{D_{Sc}^{5/4}}{(2h_0)^{5/4}}\left(\frac{8\Gamma}{\Gamma_0}\right)^{9/4}\right].\end{aligned} \tag{15}$$

The interaction energy between two unequal spheres can be obtained from that of equal spheres by the following relationship (Napper, 1983):

$$V_S(h, r_{0_k}, r_{0_l}) = \frac{2r_{0_l}}{r_{0_k} + r_{0_l}} V_S^{ES}(h, r_{0_k}). \tag{16}$$

V_S^{ES} is first derived by substituting V_S^{FP} in Eq. (15) into Eq. (14) and integrating. It is then substituted into Eq. (16) to obtain the following equation for interaction energy between two unequal polymer-coated spheres:

$$\begin{aligned}V_S = &\left(\frac{2\pi r_{0_k} r_{0_l}}{r_{0_k} + r_{0_l}}\right)\left(\frac{\alpha_{Sc}k_BT}{a_m^3}\right)\Phi_{s0}^{9/4}D_{Sc} \\ &\times\left\{-\frac{16\Gamma D_{sc}}{\Gamma_0}\ln\left(\frac{2\delta}{h_0}\right) + \frac{4D_{Sc}^{5/4}}{2^{5/4}}\left(\frac{8\Gamma}{\Gamma_0}\right)^{9/4}\right. \\ &\left.\times\left[\frac{1}{h_0^{1/4}} - \frac{1}{(2\delta)^{1/4}}\right]\right\}.\end{aligned} \tag{17}$$

The first term within the curly brackets in Eq. (17) represents short-range attraction while the second term accounts for excluded volume repulsion. The relative magnitudes of these two contributions determine whether polymer adsorption results in bridging attraction or steric repulsion.

3. Results

The model was tested with experimental data for bridging flocculation (Biggs et al., 2000). These authors reported size distribution data for polystyrene latex flocs produced by using a high molecular weight (16×10^6 g/mol) cationic quaternary ammonium based derivative of polyacrylamide. The mean radius of primary particles was 165 nm and solids concentration was 0.05% w/w, which corresponds to a particle number concentration of approximately $2.53 \times 10^{16}\,\mathrm{m}^{-3}$.

All experiments were carried out at pH 6 in 10^{-4} M KNO_3 solutions in two steps. In first step, latex dispersion was vigorously stirred with a magnetic stirrer for 60 s, after the addition of the polymer. In second step, the partially flocculated suspension was transferred to a light scattering cell and flocculation was allowed to proceed under perikinetic aggregation conditions. The model presented here simulates the second stage as perikinetic aggregation coupled with differential sedimentation. The discretized PBE was divided into 30 geometric sections and solved numerically by Gear's predictor–corrector technique (Gear, 1971) for nonlinear ordinary differential equations. The stability ratio in Eq. (6) was evaluated by numerical integration using the Romberg algorithm (Press et al., 1992). During integration of population balance equations, the computed FSD was tested at each time step for conservation of solid volume. The loss of total solid volume was less than 1% for the results presented here.

The model involves a number of parameters, which can be measured experimentally or, in principle, calculated theoretically. These are mostly related to various particle interaction energies described in the previous section, except for mass fractal dimension of the aggregate, which is required to estimate the collision frequency factor. In case values of model parameters were not reported, representative values were taken from literature and adjusted by trial and error to match the experimental FSD data. Although parameter estimation could have been done by a suitable optimization technique, this would have resulted in a blind search without regard to practical values observed experimentally. Moreover, there was always a possibility of acquiring optimum but physically unrealistic parameter values due to mutual compensation in the highly nonlinear environment of model equation. It was ensured in the first place that values assigned to various parameters in the total interaction energy lead to attraction between particles in order to conform with the experimental conditions. Subsequently, the floc fractal dimension alone was adjusted by trial and error to obtain a closer agreement between computed and experimental FSD. The Hamaker constants of polystyrene, water and polyacrylamide across a vacuum were taken as 6.6×10^{-20}, 3.7×10^{-20} and 8×10^{-20} J, respectively (Vincent, 1973; Israelachvili, 1991). The parameters in the equation for interaction energy due to adsorbed polymer layers can be obtained from measurements with the surface forces apparatus or the atomic force microscope on forces between polymer-coated surfaces and from neutron scattering experiments on polymer volume fraction profiles. A value of 3×10^5 N/m^2 was assigned to the term $\alpha_{Sc} k_B T / a_m^3$ in Eq. (17), as reported by Klein and Rossi (1998). They obtained this value by fitting the scaling theory to the forces measured between polyethylene oxide (PEO)-coated mica surfaces. Cosgrove et al. (1990) measured volume fraction profiles of PEO on polystyrene surfaces using neutron scattering experiments and found D_{Sc} to be in the range of 3–5 nm. The polymer volume fraction at saturation, Φ_{S_0} was around 0.3. A value of 4 nm is used here for D_{Sc}. Though these values are for a different polymer-substrate system, we have assumed them to be applicable to the present system also. In order to check the validity of assigned values, interaction energies were computed between two polymer-coated particles having identical radii of 165 nm. The parameters ψ_0, Φ_{S_0} and Γ/Γ_0 were adjusted such that there is net attraction due to polymer bridging even when there is a significant electrostatic repulsion. The adsorbed layer thickness δ was also adjusted so that the polymer extends beyond the range over which electrostatic repulsion acts. After some trials, the values of ψ_0, Φ_{S_0}, Γ/Γ_0 and δ were obtained as -31 mV, 0.21, 0.475 and 60 nm, respectively, which are eminently reasonable.

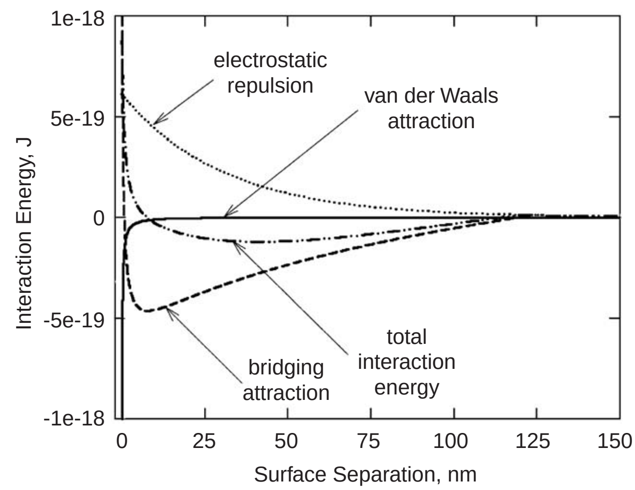

Fig. 3. van der Waals attraction (Eq. (8)), electrostatic repulsion (Eq. (10)), bridging attraction (Eq. (17)) and total interaction energy between identical spherical particles of radius 165 nm with adsorbed polymer layers, using parameter values in Table 1.

The computed interaction energy profiles are shown in Fig. 3. Under the experimental conditions and for parameter values employed, there is a net attraction due to polymer bridging. The interaction energy profiles are typical of the force-distance profiles measured between polymer-covered surfaces. Due to the low electrolyte concentration, the double layer thickness is quite large. However, bridging attraction is also present due to the adsorbed polymer. It is weakly attractive at long distances and becomes progressively stronger as the particles approach closer. The particle surfaces repel each other at very short distances due to the compression of the adsorbed layer. Even though electrostatic repulsion is present, bridging attraction dominates and results in net attraction.

The primary aggregates, obtained after magnetic stirring, were assumed to be the starting material for simulating the second stage of flocculation. The mean size of these primary aggregates was computed using the published FSD data (Biggs et al., 2000) at 2 min and used as the initial condition to predict the evolution of FSD with time. However,

Table 1
Model parameters and their values used in simulations

Parameter	Value
Hamaker constant of polystyrene across a vacuum, A_p	6.6×10^{-20} J
Hamaker constant of water across a vacuum, A_m	3.7×10^{-20} J
Hamaker constant of polyacrylamide across a vacuum, A_s	8.0×10^{-20} J
Solid–liquid interface potential, ψ_0	-31 mV
Polymer volume fraction at a single saturated surface, Φ_{s_0}	0.21
Scaling length, D_{Sc}	4 nm
Lumped parameter in Eq. (17), $\alpha_{Sc} k_B T / a_m^3$	3.0×10^5 N/m^2
Adsorbed polymer layer thickness, δ	60 nm
Fractional polymer surface coverage, Γ/Γ_0	0.475

All the parameter values are fixed and do not change during simulation.

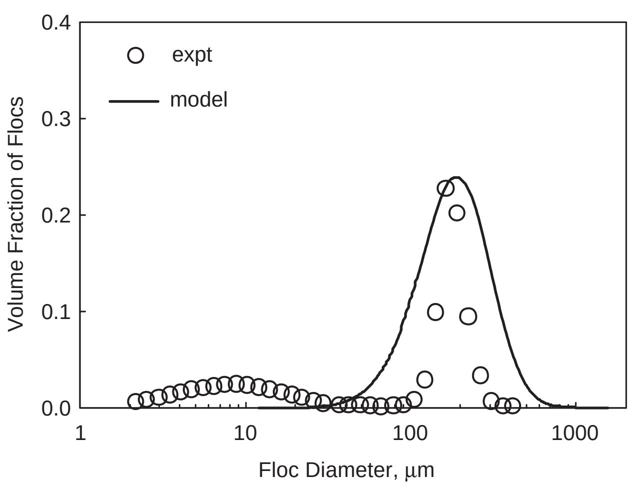

Fig. 4. Comparison of simulated and experimental size distributions of polystyrene latex flocs obtained after 10 min of flocculation using 20 ppm cationic quaternary ammonium based derivative of polyacrylamide (floc fractal dimension 1.75, mean diameter of primary aggregates 8.5 μm, parameters in Table 1). Data from Biggs et al. (2000).

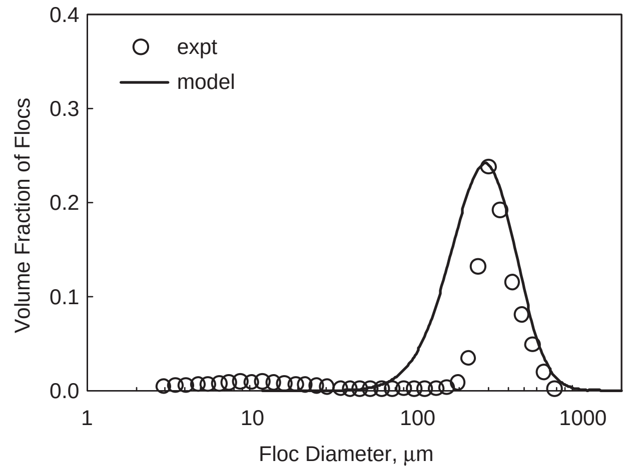

Fig. 5. Comparison of simulated and experimental size distributions of polystyrene latex flocs obtained after 30 min of flocculation using 20 ppm cationic quaternary ammonium based derivative of polyacrylamide (floc fractal dimension 1.75, mean diameter of primary aggregates 8.5 μm, parameters in Table 1). Data from Biggs et al. (2000).

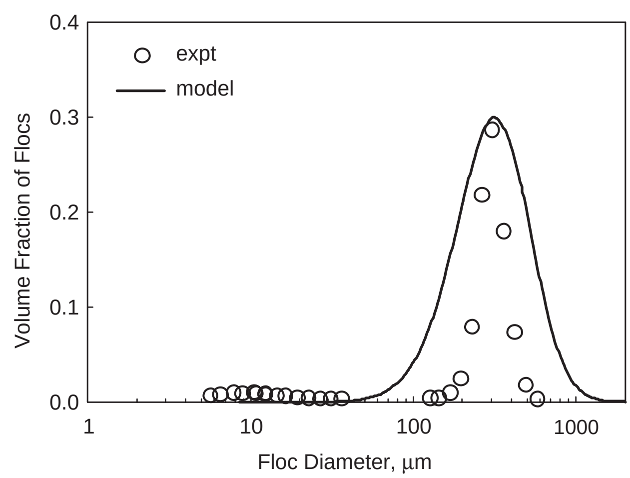

Fig. 6. Comparison of simulated and experimental size distributions of polystyrene latex flocs obtained after 30 min of flocculation using 50 ppm cationic quaternary ammonium-based derivative of polyacrylamide (floc fractal dimension 1.9, mean diameter of primary aggregates 10 μm, parameters in Table 1). Data from Biggs et al. (2000).

for computing the stability ratio in Eq. (6), r_{0_k} and r_{0_l} were set equal to 165 nm because the primary particles in the experiments of Biggs et al. (2000) were monodisperse. Similarly, surface potentials, ψ_{0_k} and ψ_{0_l} were set equal to an identical value of -31 mV because the experiments involved a single component, that is, polystyrene latex only. Glover et al. (2000) reported a value of 1.85 for fractal dimension of alumina flocs produced by bridging flocculation with a mixture of polyacrylamide and polyacrylic acid. This value was used as the initial guess and adjusted subsequently if required. The list of model parameters and their values are summarized in Table 1.

The computed results obtained using the population balance model are compared in Figs. 4 and 5 with experimental FSD at 20 ppm polymer concentration, measured after 10 and 30 min of flocculation, respectively. Although the model predicts broader FSD than the experimental data, it simulates the dynamic behavior of the process reasonably well. This is indicated by the close agreement between computed and measured peaks of the size distributions in both 10 and 30 min data. The model was also tested with data obtained at different polymer concentrations. Results obtained at 50 ppm polymer concentration are shown in Fig. 6 and it can be seen that the model predictions are close to experimental data. The simulated FSD, however, does not contain a long tail as observed in the experimental data. This could be because of the assumption of monodisperse primary aggregates in simulation, whereas in reality they possess a broad distribution. The primary aggregate size distribution could not be

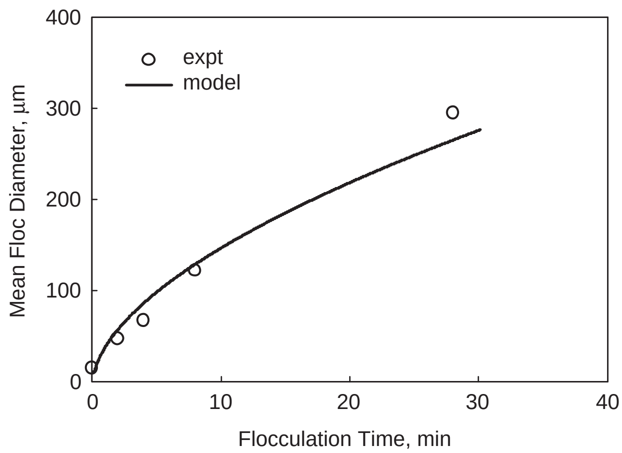

Fig. 7. Comparison of simulated and experimental time evolution of mean floc diameter with 20 ppm polymer concentration. (Floc fractal dimension 1.75, mean diameter of primary aggregates 8.5 μm, parameters in Table 1.) Data from Biggs et al. (2000).

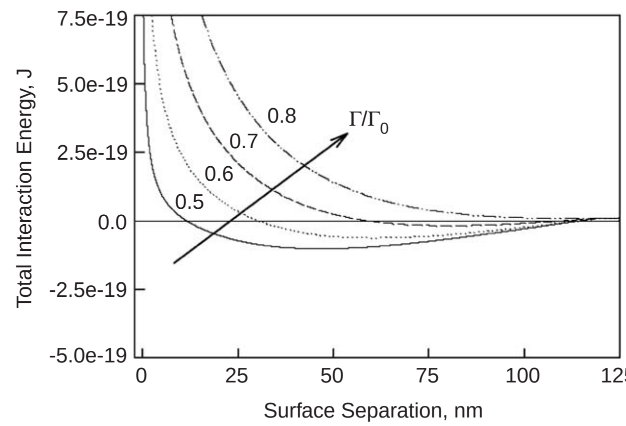

Fig. 8. Effect of Γ/Γ_0 on total interaction energy. Parameters in Table 1.

simulated because the suspension was initially stirred with a magnetic stirrer for 60 s before it was allowed to flocculate under perikinetic aggregation conditions (Biggs et al., 2000). It is difficult to associate any quantifiable shear rate for the first stage flocculation involving magnetic stirring. It is possible to obtain a better agreement between measured and predicted FSD, as for example, by assuming some arbitrary distribution of primary aggregates or by assigning different particle surface potentials or fractional surface coverages for particles/aggregates of different sizes. We however felt that such modifications at fine tuning the model would have been perceived, and rightly so, as an exercise in force fitting of data.

In order to test the model for dynamics of flocculation at a different level, simulation results were compared in Fig. 7 with experimental data for time evolution of mean floc diameter at 20 ppm polymer concentration. The arithmetic mean floc diameter d_{am} was computed from the measured FSD data reported in Fig. 2 of Biggs et al. (2000) using the following equation:

$$d_{am} = \sum_i \bar{d}_i v_i, \tag{18}$$

where $\bar{d}_i$ is arithmetic mean diameter of flocs in size class i and v_i is floc volume fraction in the same size class. It will be seen that the simulation results follow the experimental trend closely.

As mentioned earlier, the collision frequency factor was taken as a sum of contributions due to perikinetic aggregation and differential sedimentation of flocs. The contribution of latter mechanism is relatively small in case of polystyrene flocs. This is because the density of polystyrene particles is close to that of water and floc density decreases with increase in size.

4. Discussion

In spite of its complexity, the model predicts experimental trends of bridging flocculation reasonably well. This is probably due to the fact that the parameter values were obtained, wherever possible, from relevant experimental data rather than from a “blind” optimization search or nonlinear fit. Moreover, all the parameters are physically meaningful and can be accessed experimentally. They were also checked for their validity by computing the interaction forces that could probably be acting under the prevailing experimental conditions. In fact, it is advisable to check the interaction forces from the experimental data and the proposed parameter values before proceeding with simulation as the force–distance profiles should reveal the nature of these forces at the interface and indicate whether there exists a strong or weak net attraction or repulsion. It was already shown in Fig. 3 that the net interaction is attractive at fractional surface coverage of polymer chains $\Gamma/\Gamma_0 = 0.475$. Results of calculations for varying Γ/Γ_0 are given in Fig. 8, which shows that the interaction becomes repulsive as Γ/Γ_0 increases. It is well known that an optimum polymer concentration exists for flocculation of colloidal suspensions (Dobias, 1993). At low polymer concentrations, rate of flocculation is slow because electrical double layer repulsion dominates particle interactions. As polymer concentration increases, rate of flocculation increases due to charge neutralization or bridging and attains a maximum. At still higher polymer concentrations, the suspension becomes stable again because particle surfaces are saturated with polymer molecules and steric repulsion between polymer chains dominates particle interactions.

The discrepancies between simulation results and experimental FSD data could be due to several reasons, apart from those discussed earlier. One, there is some uncertainty in FSD data of Malvern Mastersizer employed in these experiments. This instrument works on the premise that flocs are solid spheres whereas in reality they are highly porous and irregularly shaped fractal objects. This is one of the main difficulties in validating population balance models of flocculation with FSD data, even though it is possible to predict the evolution of mean floc size reasonably accurately (Flesch et al., 1999; Thill et al., 2001; Biggs and Lant, 2002). Since the agreement does not improve when floc volume fraction is normalized with the corresponding section width, we have compared non-normalized volume fraction, as reported by Biggs et al. (2000). Two, no cognizance is taken of the porosity of flocs, even though we recognize that incorporation of floc porosity could possibly lead to improved estimation of collision frequency factor. Unfortunately, no relevant theoretical framework exits for tracking floc porosity in course of aggregation. Three, in order to simplify the mathematical treatment, it was assumed that polymer adsorption occurs uniformly on all particles in suspension and parameters such as particle surface potential, fractional surface coverage and adsorbed layer thickness were identical for all particles. In reality, disproportionate and nonuniform surface coverage of particles/aggregates with polymer chains occurs, resulting in a distribution of rates of aggregation on this count also. Moreover, it is extremely difficult to characterize accurately the electrochemical nature of particle surfaces in the presence of adsorbed polymer. Four, another plausible reason for model discrepancy could be due to choice of the geometric sections for grouping size classes. Lumping of size classes uniformly or by using a finer grid could conceivably result in a more accurate computation of the complete FSD. This approach, however, will be computationally more intensive than geometric lumping used in the present work, and in some cases, can lead to inaccurate solutions. For example, it was shown (Vanni, 2000) that the variable grid discretization technique of Litster et al. (1995), which is an extension of the method of Hounslow et al. (1988), generates physically meaningless sections and results in spurious oscillating components in the particle size distribution under some circumstances when finer sections are employed. Similarly, Kumar and Ramkrishna (1996) showed that it is necessary to decrease the grid spacing factor to as low as 1.15 in order to obtain good agreement between numerical and analytical solutions for aggregate size distribution. It would seem that a very fine grid, almost resembling a uniform grid, is required to accurately predict the FSD. In other words, there is a trade-off between solution accuracy and computational demand. The technique of Hounslow et al. (1988) is applied here mainly because it is robust, provides fairly accurate estimates of aggregate size distribution and more importantly, it has been tested extensively in the literature for a variety of different systems. It is, however, acknowledged that the adaptive discretization technique of Kumar and Ramkrishna (1996) could also be employed for modeling flocculation without compromising robustness or accuracy of solution.

It was assumed that polymer adsorption attains equilibrium before collisions occur between coated particles. Though this may not be a serious limitation in predicting steady-state FSD, it would be necessary to incorporate the kinetics of polymer adsorption and the dynamics of particle–polymer interactions, in order to predict the short-term flocculation kinetics. Finally, even though the model is applicable for flocculation in absence of shear, it can be readily extended to a shearing regime by including additional terms in the PBE and incorporating appropriate floc fragmentation kinetics.

5. Conclusions

Mathematical modeling of flocculation in presence of polymers requires incorporation of models for polymer-induced forces in order to predict the evolution of floc size distribution as a function of variables such as pH, electrolyte concentration, polymer molecular weight and its concentration. Flocculation models proposed previously ignore the influence of surface forces and treat collision efficiency factor as a fitting parameter. An attempt is made in the present work to integrate the theories of surface forces in presence of polymers with the population balance framework to model polymer-induced flocculation. The collision efficiency was estimated as a function of van der Waals attraction, electrical double layer repulsion and bridging attraction or steric repulsion. The model was tested with experimental floc size distribution data published in the literature and model predictions were found to reflect experimental results adequately. The present work represents the first attempt towards development of a rigorous population balance model for bridging flocculation and the reported results indicate the possibility of predicting floc size distribution as a function of input process variables under different operating conditions. Moreover, because it is computationally less demanding, this model is highly suited for on-line optimization and control of industrial flocculation processes.

Acknowledgements

This work was supported by the National Science Foundation (NSF Grants # INT-96-05197 and INT-01-17622) and the NSF Industry/University Cooperative Research Center (IUCRC) for Advanced Studies in Novel Surfactants at Columbia University (NSF Grant # EEC-98-04618). The authors thank the management of Tata Research Development and Design Centre for the permission to publish this paper. VR thanks Prof. E.C. Subbarao, Prof. Mathai Joseph and Dr. Pradip for their advice and encouragement.

References

Bell, G.M., Levine, S., McCartney, L.N., 1970. Approximate methods of determining the double-layer free energy of interaction between two charged colloidal spheres. Journal of Colloid and Interface Science 33, 335–359.

Biggs, C.A., Lant, P.A., 2002. Modeling activated sludge flocculation using population balances. Powder Technology 124, 201–211.

Biggs, S., Habgood, M., Jameson, G.J., Yan, Y.-d., 2000. Aggregate structures formed via a bridging flocculation mechanism. Chemical Engineering Journal 80, 13–22.

Camp, T.R., Stein, P.C., 1943. Velocity gradients and internal work in fluid motion. Journal of Boston Society of Civil Engineers 30, 219–237.

Cohen Stuart, M.A., Fleer, G.J., 1996. Adsorbed polymer layers in nonequilibrium situations. Annual Reviews of Materials Science 26, 463–500.

Cosgrove, T., Crowley, T.L., Ryan, K., Webster, J.R.P., 1990. The effects of solvency on the structure of an adsorbed polymer layer and dispersion stability. Colloids and Surfaces A 51, 255–269.

de Gennes, P.G., 1981. Polymer solutions near an interface. 1. Adsorption and depletion layers. Macromolecules 14, 1637–1644.

de Gennes, P.G., 1982. Polymer solutions near an interface. 2. Interaction between two plates carrying adsorbed polymer layers. Macromolecules 15, 492–500.

Derjaguin, B.V., 1934. Friction and adhesion. IV. The theory of adhesion of small particles. Kolloid-Z 69, 155–164.

Derjaguin, B.V., Muller, V.M., 1967. Slow coagulation of hydrophobic colloids. Dokl. Akad. Nauk SSSR 176, 738–741.

Dobias, B., 1993. Coagulation and Flocculation: Theory and Applications. Marcel Dekker, Inc., New York.

Firth, B.A., Hunter, R.J., 1976. Flow properties of coagulated colloidal suspensions I. Energy dissipation in the flow units. Journal of Colloid and Interface Science 57, 248–256.

Fleer, G.J., Cohen Stuart, M.A., Scheutjens, J.M.H.M., Cosgrove, T., Vincent, B., 1993. Polymers at Interfaces. Chapman & Hall, Inc., New York.

Flesch, J.C., Spicer, P.T., Pratsinis, S.E., 1999. Laminar and turbulent shear-induced flocculation of fractal aggregates. American Institute of Chemical Engineers Journal 45, 1114–1124.

Fuchs, N., 1934. Ueber die stabilitat und aufladung der aerosole. Zeitschrift fur Physik 89, 736–743.

Gear, C.W., 1971. Numerical Initial Value Problems in Ordinary Differential Equations. Prentice-Hall, Englewood Cliffs NJ, USA.

Glover, S.M., Yan, Y.-d., Jameson, G.J., Biggs, S., 2000. Bridging flocculation studied by light scattering and settling. Chemical Engineering Journal 80, 3–12.

Gregory, J., 1981. Approximate expressions for retarded van der Waals interaction. Journal of Colloid and Interface Science 83, 138–145.

Gregory, J., 1988. Polymer adsorption and flocculation in sheared suspensions. Colloids and Surfaces A 31, 231–253.

Hamaker, H.C., 1937. The London-van der Waals attraction between spherical particles. Physica IV, 1058–1072.

Honig, E.P., Roebersen, G.J., Wiersema, P.H., 1971. Effect of hydrodynamic interaction on the coagulation rate of hydrophobic colloids. Journal of Colloid and Interface Science 36, 97–109.

Hounslow, M.J., Ryall, R.L., Marshall, V.R., 1988. A discretized population balance for nucleation, growth, and aggregation. American Institute of Chemical Engineers Journal 34, 1821–1832.

Israelachvili, J.N., 1991. Intermolecular and Surface Forces. second ed. Academic Press, New York.

Jiang, Q., Logan, B.E., 1991. Fractal dimensions of aggregates determined from steady-state size distributions. Environmental Science and Technology 25, 2031–2038.

Klein, J., Rossi, G., 1998. Analysis of the experimental implications of the scaling theory of polymer adsorption. Macromolecules 31, 1979–1988.

Klimpel, R.C., Hogg, R., 1986. Effects of flocculation conditions on agglomerate structure. Journal of Colloid and Interface Science 113, 121–131.

Levine, S., Friesen, W.I., 1987. Flocculation of colloid particles by water-soluble polymers. In: Attia, Y.A. (Ed.), Flocculation in Biotechnology and Separation Systems. Elsevier, Amsterdam, pp. 3–20.

McGown, D.N., Parfitt, G.D., 1967. Improved theoretical calculation of the stability ratio for colloidal systems. The Journal of Physical Chemistry 71, 449–450.

Napper, D.H., 1983. Polymeric Stabilization of Colloidal Dispersions. Academic Press, Inc., New York.

Pelton, R.H., 1999. Polymer-colloid interactions in pulp and paper manufacture. In: Farinato, R.S., Dubin, P.L. (Eds.), Colloid-Polymer Interactions: From Fundamentals to Practice. Wiley, New York, pp. 51–82.

Press, W.H., Teukolsky, S.A., Vetterling, W.T., Flannery, B.P., 1992. Numerical Recipes in FORTRAN: The Art of Scientific Computing. second ed. Cambridge University Press, New York.

Runkana, V., 2003. Mathematical modeling of flocculation and dispersion of colloidal suspensions. D.E.Sc. Thesis, Columbia University, New York.

Runkana, V., Somasundaran, P., Kapur, P.C., 2004. Mathematical modeling of polymer-induced flocculation by charge neutralization. Journal of Colloid and Interface Science 270, 347–358.

Smoluchowski, M.v., 1916. Drei vortrage uber diffusion, Brownsche molekularbewegung und koagulation vor kolloidteilchen. Physikalische Zeitschrift 17, 557–571.

Somasundaran, P., Das, K.K., Yu, X., 1996. Selective flocculation. Current Opinion in Colloid and Interface Science 1, 530–534.

Spicer, P.T., Pratsinis, S.E., 1996. Coagulation and fragmentation: universal steady-state particle-size distribution. American Institute of Chemical Engineers Journal 42, 1612–1620.

Spielman, L.A., 1970. Viscous interactions in Brownian coagulation. Journal of Colloid and Interface Science 33, 562–571.

Thill, A., Moustier, S., Aziz, J., Wiesner, M.R., Bottero, J.Y., 2001. Flocs restructuring during aggregation: experimental evidence and numerical simulation. Journal of Colloid and Interface Science 243, 171–182.

Thomas, D.N., Judd, S.J., Fawcett, N., 1999. Flocculation modeling: a review. Water Research 33, 1579–1592.

Tjipangandjara, K., Huang, Y.-B., Somasundaran, P., Turro, N.J., 1990. Correlation of alumina flocculation with adsorbed polyacrylic acid conformation. Colloids and Surfaces A 44, 229–236.

van de Ven, Theo G.M., 1994. Kinetic aspects of polymer and polyelectrolyte adsorption on surfaces. Advances in Colloid and Interface Science 48, 121–140.

Vanni, M., 2000. Approximate population balance equations for aggregation-breakage processes. Journal of Colloid and Interface Science 221, 143–160.

Vincent, B., 1973. The van der Waals attraction between colloid particles having adsorbed layers. II. Calculation of interaction curves. Journal of Colloid and Interface Science 42, 270–285.

Vold, M.J., 1961. The effect of adsorption on the van der Waals interaction of spherical colloidal particles. Journal of Colloid and Interface Science 16, 1–12.

Yu, X., Somasundaran, P., 1996. Role of polymer conformation in interparticle-bridging dominated flocculation. Journal of Colloid and Interface Science 177, 283–287.

Zhang, J., Buffle, J., 1995. Kinetics of hematite aggregation by polyacrylic acid: importance of charge neutralization. Journal of Colloid and Interface Science 174, 500–509.